International Journal of Medical Toxicology & Forensic Medicine
2026, Volume 16, E52682

Research Paper

Hepatotoxic Effects of Biosynthesized Zinc Oxide Nanoparticles and Bulk ZnO: Protective Role of *Allium sativum* Extract in Male Albino Rats

Malak Fadil Hwaidi*, **Shaimaa Hussein Ali**, **Sura A. Awadh**

Department of Biology, College of Science, Al-Qasim Green University, Babylon, Iraq.

Citation Hwaidi MF, Ali ShH, Awadh SA. Hepatotoxic Effects of Biosynthesized Zinc Oxide Nanoparticles and Bulk ZnO: Protective Role of *Allium sativum* Extract in Male Albino Rats. International Journal of Medical Toxicology and Forensic Medicine. 2026; 16:E52682.

https://doi.org/10.22037/ijmtfm.v16.52682

Article info:
Received: 01 July, 2026
Accepted: 15 July, 2026
Published: 15 August, 2026

Keywords:
Allium sativum, Apoptosis, Hepatotoxicity, Nanoparticles, Oxidative stress, Rats

ABSTRACT

Background: Zinc oxide nanoparticles (ZnO NPs) exhibit heightened surface reactivity, raising hepatotoxicity concerns driven by oxidative stress and apoptosis. Green synthesis using *Allium sativum* (garlic) extract is an eco-friendly alternative, yet a critical gap persists: the extract's independent biological role remains unexamined. This study comparatively evaluated the hepatic toxicity of bulk zinc oxide (Bulk ZnO) and garlic-synthesized nanoparticles, while isolating the independent biological effect of the botanical extract. The inclusion of an extract-only group is a key novelty of this study, allowing for the differentiation between the intrinsic toxicity of the nanoparticles and the potential protective effects of the synthesis medium.

Methods: Nanoparticles were biosynthesized and characterized. Eighty male albino rats were divided into eight groups (n=10) receiving oral administration for 28 days: control, extract alone, bulk zinc oxide (400, 200, 100 mg/kg), and nanoparticles (400, 200, 100 mg/kg). Hepatic enzymes, oxidative stress, and apoptotic markers were quantified.

Results: Nanoparticles induced dose-dependent hepatotoxicity significantly exceeding that of bulk equivalents. The highest elevation of oxidative stress parameters, including MDA, and the lowest SOD occurred in the highest nanoparticle dose group, accompanied by exclusive mortalities. Furthermore, hepatic injury markers (ALT, AST, ALP, and bilirubin) were significantly elevated in this group. Specifically, ALT increased to a maximum of 75.74 ± 0.33 IU/L and AST to 82.23 ± 1.86 IU/L in the high-dose nanoparticle group. Conversely, the botanical extract-alone group displayed a highly favorable profile, with reduced caspase-3 and caspase-9 and improved antioxidant capacity.

Conclusion: The observed hepatotoxicity is driven by the nanoparticulate form, not the synthesis medium. The extract independently conferred hepatoprotection. Rigorous preclinical safety evaluations of green-synthesized nanomaterials are imperative before biomedical application.

*** Corresponding Author:**
Malak Fadil Hwaidi, PhD
Department of Biology, College of Science, Al-Qasim Green University, Babylon, Iraq.
E-mail: *malak.fadil@science.uoqasim.edu.iq*

Introduction

Zinc oxide (ZnO) possesses unique physical, chemical, and economic properties that have established its widespread industrial relevance [1]. In recent years, the transition from bulk materials to nanotechnology has led to the extensive application of zinc oxide nanoparticles (ZnO NPs) in various fields, including biomedicine, cosmetics, electronics, UV-absorbing packaging, and agriculture [2]. Nanoparticles, typically defined as having dimensions between 1 and 100 nm, exhibit a remarkably high surface-area-to-volume ratio compared to their bulk counterparts. This unique structural feature significantly enhances their biological reactivity and facilitates the generation of reactive oxygen species (ROS), thereby raising substantial biosafety and toxicological concerns [3]. Despite their expanding utilization, comprehensive toxicological evaluations of ZnO NPs remain incomplete, necessitating rigorous in vivo investigations [4].

Conventional methods for synthesizing nanoparticles often rely on toxic chemicals and high-energy processes, which limit their scalability and pose environmental risks. Consequently, green synthesis has emerged as a sustainable and biocompatible alternative, utilizing plant phytochemicals as natural reducing and stabilizing agents [5]. Among various botanical candidates, garlic (*Allium sativum*) is particularly attractive for nanoparticle synthesis due to its rich composition of bioactive constituents, including allicin, alliin, diallyl sulfides, ajoene, and S-allyl cysteine [6]. These phytochemicals are well-documented for their antioxidant, anti-inflammatory, hepatoprotective, and broad pharmacological effects [7] Plant-derived extracts generally share convergent protective mechanisms, including enhanced antioxidant defense, suppression of inflammatory responses, and inhibition of apoptotic pathways [8]. However, the biological activity of garlic is complex; while it offers protective benefits, high doses of garlic extract can independently induce dose-dependent hepatic alterations [9].

Following green synthesis, thorough characterization of the resulting nanoparticles is essential to confirm their successful formation, size, and purity [10]. Upon systemic exposure, the liver acts as the primary detoxification organ and sequesters approximately 80% of circulating nanoparticles [11]. Internalized ZnO NPs are known to generate excessive ROS, which overwhelms the cellular antioxidant defense mechanisms, leading to severe oxidative damage [12]. This oxidative stress manifests clinically as elevated serum hepatic enzymes, indicating hepatocellular injury [13]. Furthermore, severe and prolonged oxidative stress can trigger programmed cell death via the intrinsic mitochondrial apoptotic pathway, characterized by the activation of key executioner proteins, including caspase-3 and caspase-9 [14].

While green synthesis aims to mitigate the toxicity associated with chemical synthesis, the inherent toxicity of the nanomaterial itself, coupled with the dual biological potential of the plant extract used for synthesis, presents a complex toxicological paradigm. There is a critical gap in understanding whether the observed biological effects of green-synthesized ZnO NPs are driven by the nanoparticle core, the phytochemical capping agents, or a synergistic interaction between the two. Therefore, this study aimed to prepare garlic-mediated ZnO NPs, characterize their physicochemical properties, and comparatively evaluate the hepatic toxicity of bulk ZnO and green-synthesized ZnO NPs in a rat model, while specifically isolating and assessing the independent biological effect of the Allium sativum extract on liver enzymes, antioxidant status, and apoptotic markers.

Materials and Methods

Preparation of Garlic Extract (Allium sativum)

Fresh garlic bulbs (Allium sativum) were peeled and mechanically crushed without the addition of any solvent (e.g., distilled water). The resulting paste was filtered through sterile medical gauze to remove fibrous residues, yielding a crude, undiluted garlic juice. This cold, solvent-free extraction method was adopted to preserve the native concentration and thermostable bioactive compounds (e.g., allicin) of fresh garlic, as it avoids the heat-induced degradation associated with conventional aqueous extraction protocols that rely on dried powder boiled in water, with modifications based on the protocol described by [15]. The freshly prepared filtrate was divided into two portions: one portion was used immediately for the green synthesis of ZnO nanoparticles, and the other was reserved for direct oral administration to the experimental group (Group 2). Each rat in Group 2 received a fixed daily oral dose of 100 mg/kg of the crude undiluted garlic juice (administered in a volume of 0.3 mL based on average body weight) by gavage for 28 consecutive days. The extract was stored at −20°C until use, and fresh batches were prepared whenever the stored volume was depleted.

Green Synthesis of Zinc Oxide Nanoparticles (ZnO NPs)

The green synthesis of ZnO NPs was performed using garlic extract as both a reducing and capping agent, adapted from the method outlined by [16]. Zinc acetate dihydrate (0.7, 1.5, and 3.0 g) was dissolved in

50 mL deionized water to obtain target doses of 100, 200, and 400 mg/kg, respectively. These doses were selected based on previous nanotoxicological studies to evaluate potential environmental and biomedical exposure scenarios. Although the oral LD_{50} of ZnO NPs in rodents exceeds 2,000 mg/kg [17], sub-acute toxicity has been reported at doses above 200 mg/kg [18]. Therefore, the chosen range (100-400 mg/kg) allows for the assessment of both well-tolerated and potentially toxic dose levels. In the present study, both 200 and 400 mg/kg doses caused mortality, with the 400 mg/kg dose being considerably more lethal; the 100 mg/kg dose was well tolerated. The solution was heated to 50–60 °C with stirring, and garlic extract was added dropwise until a white precipitate formed (~30 min), then concentrated at 90–100 °C. The final nanosuspension was adjusted to a total volume sufficient for the entire 28-day study period for all animals in the respective groups, ensuring a consistent concentration. The actual administration volume given to each mouse daily was calculated based on its body weight (e.g., 1.5 mL/kg of body weight) to deliver the exact target doses (100, 200, or 400 mg/kg). An aliquot was oven-dried at 100 °C for characterization.

Characterization of Zinc Oxide Nanoparticles

The biosynthesized ZnO NPs were characterized to confirm their structural and morphological properties. Fourier Transform Infrared (FTIR) spectroscopy was utilized to identify the functional groups and phytochemical capping on the nanoparticle surface. Field Emission Scanning Electron Microscopy (FESEM) was employed to determine the surface morphology and size distribution. Energy Dispersive X-ray (EDX) spectroscopy was conducted to verify the elemental composition and purity of the synthesized nanoparticles. All characterization analyses were performed via the BPC Analysis Center (Baghdad, Iraq) at an affiliated facility in Iran.

Preparation of Bulk ZnO Suspension

Commercially available bulk ZnO powder (Fluka, Switzerland) was suspended in 5 mL of deionized water. For the respective dose groups of 100, 200, and 400 mg/kg, 0.250 g, 0.500 g, and 1.0 g of bulk ZnO were used. The suspensions were thoroughly mixed before oral administration.

Animals and Experimental Design

Eighty healthy male albino rats, aged 2–3 months and weighing between 150 and 250 g, were procured and housed under standard controlled environmental conditions (temperature: 22–25 °C; 12-hour light/dark cycle; free access to food and water) at the animal house facility of Babylon University. Following a one-week acclimatization period, the rats were randomly allocated into eight equal groups (n = 10 per group) as outlined in Table 1.

All treatments were administered daily via oral gavage for a consecutive period of 28 days. The study protocol was approved by the institutional animal ethics committee of Al-Qasim Green University.

Table 1. Experimental grouping and treatment design of rats.

Groups	Treatments
1	Received standard diet and water without any treatment
2	Received 100 mg/kg (0.3 mL/day) of freshly prepared undiluted garlic extract
3	Received bulk ZnO at a dose of 400 mg/kg
4	Received bulk ZnO at a dose of 200 mg/kg
5	Received bulk ZnO at a dose of 100 mg/kg
6	Received green-synthesized ZnO NPs at a dose of 400 mg/kg
7	Received green-synthesized ZnO NPs at a dose of 200 mg/kg
8	Received green-synthesized ZnO NPs at a dose of 100 mg/kg

International Journal of
Medical Toxicology & Forensic Medicine

Sample Collection

On day 29, following the 28-day treatment period, all surviving rats were euthanized using chloroform anesthesia. Blood samples were collected via cardiac puncture into gel-separator tubes. The blood was allowed to clot at room temperature and then centrifuged at 5000 rpm for 10 minutes to separate the serum, which was carefully aliquoted and stored at −20 °C for subsequent biochemical analyses. Liver tissues were promptly excised, rinsed with cold physiological saline (0.9% NaCl) to remove excess blood, and homogenized in phosphate-buffered saline (PBS, pH 7.4). The homogenates were centrifuged at 3000 rpm for 10 minutes, and the resulting supernatants were collected and stored at −20 °C for the quantification of tissue biomarkers.

Biochemical Parameters

Oxidative Stress and Apoptotic Markers

Serum levels of malondialdehyde (MDA), a marker of lipid peroxidation, and superoxide dismutase (SOD), an antioxidant enzyme, were quantified using specific rat Enzyme-Linked Immunosorbent Assay (ELISA) kits (Cat. No. E0156Ra and Cat. No. E0168Ra, respectively; Bioassay Technology Laboratory, China). The concentrations of pro-apoptotic markers, caspase-3 and caspase-9, in the liver homogenate supernatants were determined using rat ELISA kits (Cat. No. E-EL-R0160 and Cat. No. E-EL-R0163, respectively; Elabscience, China). All assays were performed strictly according to the manufacturers' protocols.

Hepatic Function Assessment

The activities of serum hepatic enzymes, including alanine aminotransferase (ALT) and aspartate aminotransferase (AST), were measured using commercial diagnostic kits (REF BS.1/PT05.010.0050 for ALT, Cat. No. BS.1/OT05.010.0050 for AST; Arena BioScien, Egypt). Alkaline phosphatase (ALP) activity was assayed using a specific kit (REF 80014; BIOLABO, France). Total bilirubin concentration in the serum was determined using a diagnostic kit (REF 80403; BIOLABO, France). All biochemical analyses were conducted following the standard procedures provided by the respective manufacturers.

Statistical Analysis

Data are expressed as the mean ± standard error (SE). Statistical comparisons among the experimental groups were performed using one-way analysis of variance (ANOVA), followed by the Least Significant Difference (LSD) post-hoc test to identify specific inter-group differences. A probability value of $P \leq 0.01$ was considered statistically significant for all comparisons.

Results

Characterization of Zinc Oxide Nanoparticles

Fourier Transform Infrared Spectroscopy

The FTIR spectrum of the biosynthesized ZnO NPs (Figure 1) revealed prominent absorption bands ranging from 3437.15 cm^{-1} to 474.49 cm^{-1}. The broad absorption band at approximately 3437 cm^{-1} corresponds to O–H stretching vibrations, indicative of hydroxyl groups from the garlic extract. The absorption band observed at 474.49 cm^{-1} is characteristic of the Zn–O stretching vibration, confirming the successful formation of the ZnO crystalline phase.

Field Emission Scanning Electron Microscopy

FESEM analysis was utilized to evaluate the morphological characteristics of the synthesized nanoparticles. The FESEM micrographs (Figure 2) demonstrated that the green-synthesized ZnO NPs were predominantly quasi-spherical in shape, with particle sizes consistently falling within the nanoscale range (sub-100 nm). The micrographs also revealed some degree of agglomeration at lower magnifications, which is a common feature of nanoparticles synthesized via green methods due to the organic capping layer.

Energy Dispersive X-ray Spectroscopy

The elemental composition of the nanoparticles was confirmed via EDX spectroscopy. The EDX spectrum (Figure 3) exhibited strong and prominent signals for Zinc (Zn) and Oxygen (O), validating the formation of ZnO. The quantitative analysis revealed weight percentages of 16.3% for Zn, 25.1% for O, and 52.6% for Carbon (C). The significant carbon content is attributed to the organic capping provided by the phytochemical constituents of the *Allium sativum* extract, which is characteristic of green-synthesized nanoparticles.

Biochemical Analysis

Oxidative Stress Markers in Serum

The administration of ZnO NPs and bulk ZnO significantly altered the systemic redox balance, as demonstrated in Table 2. Superoxide dismutase (SOD) activity was significantly elevated ($P \leq 0.01$) in the garlic extract group (G2) compared to the control, reflecting the antioxidant capacity of *Allium sativum*. Conversely, SOD activity was significantly diminished in groups treated with higher doses of bulk ZnO (G3

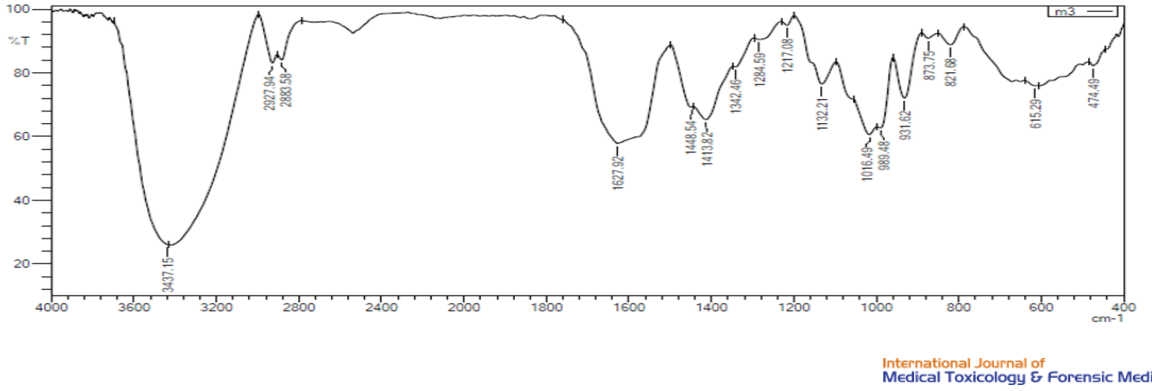

Figure 1. Fourier Transform Infrared spectrum of green-synthesized Zinc Oxide Nanoparticles utilizing *Allium sativum* (garlic) extract as a capping agent.

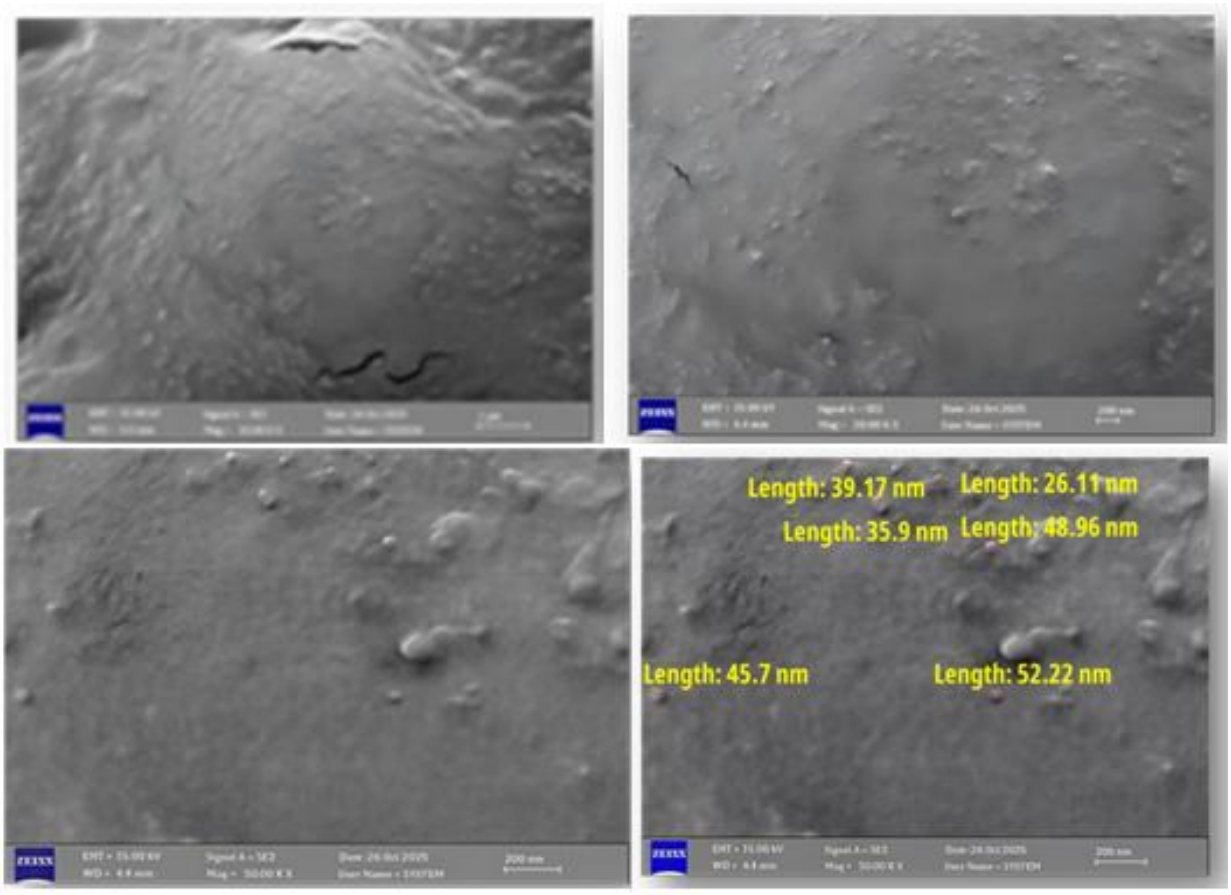

Figure 2. Field Emission Scanning Electron Microscopy micrographs demonstrating the quasi-spherical morphology and nanoscale size distribution of the green-synthesized ZnO NPs at varying magnifications.

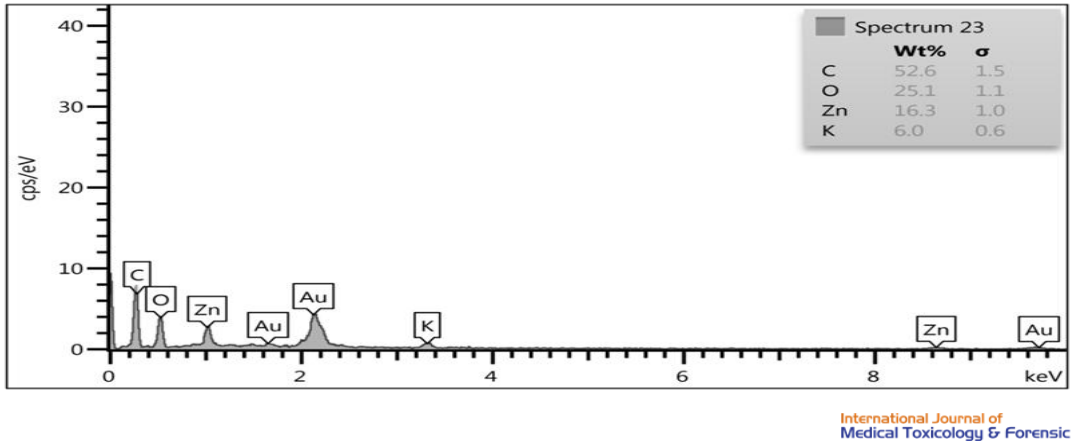

Figure 3. Energy Dispersive X-ray spectrum of the green-synthesized ZnO NPs, confirming the elemental presence of Zinc (Zn), Oxygen (O), and Carbon (C) from the organic capping agent.

and G4) and ZnO NPs (G6 and G7), indicating depletion of the antioxidant defense system under oxidative challenge. The low-dose groups (G5 and G8) showed no significant change in SOD activity relative to the control. Malondialdehyde (MDA) levels, indicative of lipid peroxidation, were significantly elevated across all treatment groups (G2–G8) compared to the control. Notably, the most profound elevation in MDA concentration was observed in the high-dose ZnO NP group (G6), indicating severe oxidative stress induced by the nanoparticulate form at the highest dose.

Apoptotic Markers (Caspase-9 and Caspase-3)

Treatment with garlic extract alone (G2) resulted in a significant decrease ($P \leq 0.01$) in both caspase-9 (14.18 ± 0.41 ng/mL) and caspase-3 (6.76 ± 0.32 ng/mL) levels

compared to the control group (16.01 ± 0.38 and 7.97 ± 0.34 ng/mL, respectively), suggesting an anti-apoptotic effect of the extract. In contrast, administration of the higher doses of bulk ZnO (G3 and G4) and ZnO NPs (G6 and G7) led to significant, dose-dependent increases in both apoptotic markers. The most substantial elevations in caspase-9 (30.88 ± 0.45 ng/mL) and caspase-3 (18.00 ± 0.43 ng/mL) were recorded in the high-dose ZnO NP group (G6) (Table 3).

Hepatic Function Enzymes

The garlic extract group (G2) demonstrated a hepatoprotective profile, characterized by significant reductions in ALT (18.73 ± 1.18 IU/L) and AST (43.07 ± 4.32 IU/L) activities compared to the control (33.49 ± 1.70 and 55.10 ± 0.51 IU/L, respectively), while ALP and total bilirubin remained unchanged. Conversely, exposure to bulk ZnO and ZnO NPs induced dose-dependent hepatic injury. ALT activity was significantly elevated in groups G3, G4, G6, G7, and G8 compared to the control. AST activity was significantly increased in groups G3, G6, and G7. ALP activity showed significant elevations in groups G3, G4, G6, G7, and G8. Total bilirubin concentrations were significantly increased in groups G3, G4, G6, and G7. Consistently across all measured hepatic function parameters, the highest levels of enzymatic leakage and bilirubin elevation were observed in the high-dose ZnO NP group (G6), with ALT reaching 75.74 ± 0.33 IU/L, AST reaching 82.23 ± 1.86 IU/L, ALP reaching 35.85 ± 1.37 IU/L, and total bilirubin reaching 0.574 ± 0.04 mg/dL (Table 4).

Discussion

The present study provides a comprehensive comparative evaluation of the hepatotoxic profiles of bulk ZnO and green-synthesized ZnO NPs, while isolating the independent biological effects of the Allium sativum extract utilized as the synthesis medium. The structural characterization of the biosynthesized ZnO NPs via FTIR, FESEM, and EDX confirmed the successful formation of nanoscale wurtzite-phase ZnO, adequately capped by phytochemical constituents. The FTIR spectrum displayed a characteristic Zn–O stretching band at 474.49 cm^{-1}, which aligns with previous reports of crystalline ZnO formation [16, 19]. The broad absorption bands spanning 821–3437 cm^{-1} correspond to the functional groups of Allium sativum metabolites, confirming their dual role as reducing and stabilizing agents [15, 20]. FESEM micrographs revealed quasi-spherical nanoparticles with sub-100 nm dimensions, while EDX analysis verified the elemental purity of the ZnO phase, alongside minor carbon peaks originating from the organic capping layer [21, 22]. These physicochemical properties are consistent with the typical profile of plant-mediated ZnO NPs, wherein the phytochemical capping prevents excessive agglomeration and enhances colloidal stability [20, 23].

The biochemical analysis revealed a profound, dose-dependent induction of oxidative stress in rats exposed to ZnO NPs, significantly exceeding the toxicity observed with equivalent doses of bulk ZnO. This differential toxicity is primarily attributable to the intrinsic physicochemical properties of nanoparticles. As delineated by Waris et al., the transition from bulk to nanoscale drastically increases the surface-area-to-volume ratio, thereby amplifying surface reactivity and facilitating excessive ROS generation at the bio-nano interface [11]. Furthermore, the enhanced hepatotoxicity of ZnO NPs can be elucidated by the "Trojan horse" mechanism. Upon systemic circulation, nanoparticles are predominantly sequestered by the liver, where they undergo cellular internalization via endocytosis. Within the acidic environment of lysosomes, ZnO NPs rapidly dissolve, releasing a massive influx of intracellular Zn^{2+} ions [24]. This intracellular dissolution overwhelms zinc homeostasis, triggering severe oxidative stress and mitochondrial dysfunction. Pei *et al*. demonstrated that the lethality of ZnO NPs surpasses conventional ZnO precisely due to this mechanism, resulting in pronounced mitochondrial damage, calcium overload, and subsequent hepatocyte necrosis [24]. In the current study, the severe depletion of SOD and marked elevation of MDA in the high-dose ZnO NP groups (G6 and G7) corroborate this mechanistic paradigm, indicating a complete overwhelming of the hepatic antioxidant defense system [4, 25]. Conversely, the low-dose groups (G5, G8) exhibited lipid peroxidation without significant SOD depletion, suggesting a biological threshold below which the cellular redox buffering capacity remains partially functional [26, 27]. This observation aligns with the concept that mild oxidative stress can be effectively neutralized by endogenous antioxidant mechanisms, including SOD, without progressing to overt cellular injury. However, as the dose increases to 200 and 400 mg/kg, this buffering capacity is progressively overwhelmed, leading to significant SOD depletion, pronounced lipid peroxidation, and subsequent hepatocyte damage [12, 24]. These findings are consistent with the established dose-dependent toxicity profile of ZnO NPs, where lower doses fall within the liver's adaptive capacity, while higher doses exceed this capacity and trigger irreversible injury cascades [7, 28].

Prolonged and severe oxidative stress inevitably culminates in programmed cell death. Our findings demonstrate a significant, dose-dependent upregulation of executioner caspases (caspase-3 and caspase-9) in

the hepatic tissues of ZnO NP-treated rats. The activation of caspase-9, an initiator caspase of the intrinsic apoptotic pathway, signifies profound mitochondrial damage. As intracellular ROS accumulate, mitochondrial membrane permeability transitions occur, leading to the release of cytochrome c and the subsequent assembly of the apoptosome, which activates caspase-9 and downstream caspase-3 [14]. The magnitude of caspase elevation was substantially higher in the ZnO NP groups compared to the bulk ZnO groups, reinforcing the heightened cytotoxicity of the nanoparticulate form [29, 30]. Recent investigations have also implicated alternative cell death pathways, such as the ROS-mediated canonical pyroptosis pathway and NLRP3 inflammasome activation, as critical targets of ZnO NP-induced liver toxicity [12, 24]. These molecular cascades collectively contribute to the severe hepatocellular injury observed in the present study, manifested clinically as the pronounced elevation of serum ALT, AST, ALP, and bilirubin levels in the nanoparticle-exposed groups [28, 31].

Crucially, the current study resolves a persistent ambiguity in green nanotechnology by isolating the biological effect of the synthesis medium. It is well established that SOD activity responds to a variety of dietary and physiological stimuli [32]. The administration of *Allium sativum* G2 elicited a highly favorable hepatic profile, characterized by significantly elevated SOD activity, decreased caspase levels, and optimal hepatic enzyme markers compared to the control. This confirms the independent hepatoprotective, antioxidant, and anti-apoptotic properties of garlic extract. Similar protective patterns have been observed with other botanical extracts, which enhance antioxidant defenses and suppress inflammatory responses, reinforcing the view that diverse plant-derived extracts share convergent cytoprotective mechanisms [33]. Therefore, the severe hepatotoxicity observed in the ZnO NP groups cannot be attributed to the residual phytochemical capping agents derived from the synthesis process. Instead, the toxicity is entirely driven by the nanoparticulate ZnO core. While green synthesis provides an eco-friendly fabrication route and the capping agents may offer localized surface passivation, this botanical functionalization is insufficient to counteract the overwhelming intracellular oxidative stress generated by the dissolved Zn^{2+} ions and the highly reactive nanoparticle surface.

Conclusion

This investigation demonstrates that the dose-dependent hepatotoxicity of green-synthesized zinc oxide nanoparticles significantly surpasses that of their bulk counterparts, driven by exacerbated oxidative stress and intrinsic apoptosis resulting from the nanoscale core. Crucially, the *Allium sativum* extract independently confers robust hepatoprotection. These findings underscore a critical toxicological paradigm: the benign nature of a green synthesis medium does not negate the intrinsic toxicity of the resulting nanomaterial. Consequently, rigorous, dose-specific preclinical safety evaluations of green-synthesized nanoparticles remain absolutely imperative prior to their translation into biomedical or clinical applications.

Ethical Approval

All experimental protocols and procedures involving animals were conducted in strict accordance with institutional and national ethical standards. The research protocol for this study ("Evaluation of Hepatic and Renal Toxicity of Zinc Oxide Nanoparticles through Biochemical and Apoptotic Enzyme Markers in Albino Rats") was reviewed and approved by the Research Ethics Committee of Al-Qasim Green University, Babylon, Iraq (Certificate No.: qgec/52/2025; Date of Approval: 27 December 2025).

Acknowledgment

None.

Funding

No external funding was received for this research.

Conflicts of Interest

The authors report there are no competing interests to declare.

References

[1] Moezzi A, McDonagh AM, Cortie MB. Zinc oxide particles: Synthesis, properties and applications. Chem Eng J. 2012;185-186:1-22. [DOI: 10.1016/j.cej.2012.01.076]

[2] Lakshmipriya T, Gopinath SCB, Rajasingam M, Arun SI, Fakhri MA, Salim ET. Advancements with Zinc Oxide Nanomaterials: From Green Chemistry to Biomedical Applications. BioNanoSci. 2026;16:310. [DOI: 10.1007/s12668-026-02549-x]

[3] Mendes AR, Granadeiro CM, Leite A, Pereira E, Teixeira P, Poças F. Optimizing antimicrobial efficacy: investigating the impact of zinc oxide nanoparticle shape and size. Nanomaterials. 2024;14(7):638. [DOI: 10.3390/nano14070638]

[4] Abouzeinab NS, Kahil N, Fakhruddin N, Awad R, Khalil MI. Intraperitoneal hepato-renal toxicity of zinc oxide and nickel oxide nanoparticles in male rats: biochemical, hematological and histopathological studies. EXCLI J. 2023;22:619-44. [DOI: 10.17179/excli2023-6237]

[5] Shahid M, Ijaz N, Shahid B, Tufail T, Ain HBU, Hussain M, Basharat S, Ikram A, Al Jbawi E. Eucalyptus globulus Labill. Mediated synthesis of ZnO nanoparticles, their optimization and characterization. Cogent Food Agric. 2024;10(1):2293332. [DOI: 10.1080/23311932.2023.2293332]

[6] Shang A, Cao SY, Xu XY, Gan RY, Tang GY, Corke H, Mavumengwana V, Li HB. Bioactive compounds and biological functions of garlic (Allium sativum L.). Foods. 2019;8(7):246. [DOI: 10.3390/foods8070246]

[7] Ozma MA, Abbasi A, Ahangarzadeh Rezaee M, Hosseini H, Hosseinzadeh N, Sabahi S, Noori SMA, Sepordeh S, Khodadadi E, Lahouty M, Kafil HS. A critical review on the nutritional and medicinal profiles of garlic's (Allium sativum L.) bioactive compounds. Food Rev Int. 2023;39(9):6324-61. [DOI: 10.1080/87559129.2022.2100417]

[8] Chabuk H, Awadh SA. Efficacy of Nigella sativa oil to relieve effects of the lead monoxide toxicity on testicular efficiency and sexual behaviour disorders in albino rats. Malays Appl Biol. 2022;51(2):41-51. [DOI: 10.55230/mabjournal.v51i2.2229]

[9] Saryono, Sarmoko, Nani D, Proverawati A, Taufik A. Black solo garlic protects hepatic and renal cell function in streptozotocin-induced rats. Front Nutr. 2022;9:962993. [DOI: 10.3389/fnut.2022.962993]

[10] Abdelbaky AS, Abd El-Mageed TA, Babalghith AO, Selim S, Mohamed AM. Green synthesis and characterization of ZnO nanoparticles using Pelargonium odoratissimum (L.) aqueous leaf extract and their antioxidant, antibacterial and anti-inflammatory activities. Antioxidants. 2022;11(8):1444. [DOI: 10.3390/antiox11081444]

[11] Waris A, Sharif S, Naz S, Manzoor F, Jamil F, Hussain M, Choi YJ, Park YK. Hepatotoxicity induced by metallic nanoparticles at the cellular level: A review. Environ Eng Res. 2023;28(5):220625. [DOI: 10.4491/eer.2022.625]

[12] Chang YN, Zhang M, Xia L, Zhang J, Xing G. The toxic effects and mechanisms of CuO and ZnO nanoparticles. Materials. 2012;5(12):2850-71. [DOI: 10.3390/ma5122850]

[13] Kahil N, Abouzeinab NS, Hussein MAA, Khalil MI. Intraperitoneal hepatorenal toxicity of zinc oxide and nickel oxide nanoparticles in rats: a systematic review. Nanotoxicology. 2024;18(7):583-98. [DOI: 10.1080/17435390.2024.2407352]

[14] Gultekin M, Eren M, Koca FD, Bozbek CK, Develi N. The effects of zinc oxide nanoparticles on the oxidative stress, caspase-3, cytokine and immunity in rats. Vet Med-Czech. 2025;70(10):379-92. [DOI: 10.17221/11/2025-VETMED]

[15] Kebede Urge S, Tiruneh Dibaba S, Belay Gemta A. Green synthesis method of ZnO nanoparticles using extracts of Zingiber officinale and garlic bulb (Allium sativum) and their synergetic effect for antibacterial activities. J Nanomater. 2023;2023:7036247. [DOI: 10.1155/2023/7036247]

[16] Lestari PP, Fitriana F, Faaizatunnisa N, Munasir M. Green synthesis of ZnO nanoparticles using garlic (Allium sativum L.) bulb extract as a photocatalyst for Congo red dye. J Phys Conf Ser. 2024;2900(1):012018. [DOI: 10.1088/1742-6596/2900/1/012018]

[17] Kong T, Zhang SH, Zhang JL, Hao XQ, Yang F, Zhang C, et al. Acute and cumulative effects of unmodified 50-nm nano-ZnO on mice. Biol Trace Elem Res. 2018;185(1):124-34. [DOI: 10.1007/s12011-017-1233-6]

[18] Pandey H, Motilal BA, Gupta D, Verma S, Verma A, Gangwar K, et al. Pathomorphological and immunological assessment of ZnO nanoparticles induced hepatic toxicity in male Wistar rats. J Anim Res. 2025;15(4):141-8. [DOI: 10.30954/2277-940X.04.2025.4]

[19] Younas MU, Iqbal M, Ahmad N, Iqbal S, Kausar A, Nazir A, et al. Biogenic synthesis of zinc oxide nanoparticles using NARC G1 garlic (Allium sativum) extract, their photocatalytic activity for dye degradation and antioxidant activity of the extract. Results Chem. 2025;13:102035. [DOI: 10.1016/j.rechem.2025.102035]

[20] Abdelmoteleb A, Valdez-Salas B, Beltran-

Partida E, Mendez-Trujillo V, González-Mendoza D, Tzintzun-Camacho O, Roumia AF. Biosynthesis of zinc oxide nanoparticles using garlic peel extract and their antibacterial potential. Microbiol Res. 2024;15(3):1655-69. [DOI: 10.3390/microb]

[21] Daimari J, Deka AK. Anticancer, antimicrobial and antioxidant activity of CuO-ZnO bimetallic nanoparticles: green synthesised from Eryngium foetidum leaf extract. Sci Rep. 2024;14:19506. [DOI: 10.1038/s41598-024-69847-w]

[22] Ogbonna CE, Kavaz D, Olawade DB, Adekunle YA. Novel green synthesis of ZnO, CaO, and ZnO-CaO hybrid nanocomposites using extract of Foeniculum vulgare (Fennel) stalks: characterization, mechanical stability, and biological activities. J Sol-Gel Sci Technol. 2025;116(1):823-35. [DOI: 10.1007/s10971-025-06863-w]

[23] Islam MF, Miah MAS, Huq AO, Saha AK, Mou ZJ, Mondol MMH, Bhuiyan MNI. Green synthesis of zinc oxide nanoparticles using Allium cepa L. waste peel extracts and its antioxidant and antibacterial activities. Heliyon. 2024;10(3):e25430. [DOI: 10.1016/j.heliyon.2024.e25430]

[24] Pei X, Jiang H, Xu G, Li C, Li D, Tang S. Lethality of zinc oxide nanoparticles surpasses conventional zinc oxide via oxidative stress, mitochondrial damage and calcium overload: a comparative hepatotoxicity study. Int J Mol Sci. 2022;23(12):6724. [DOI: 10.3390/ijms23126724]

[25] Abdallah MA, Fehaid A, Halawa AA, Ealmagd MMA. Immuno-toxic effects of zinc oxide nanoparticles and protective role of Moringa oleifera on thymus of male albino rats. Mansoura Vet Med J. 2026;26(3):3. [DOI: 10.35943/2682-2512.1260]

[26] Mirzaei F, Abbasi E, Mirzaei A, Hosseini NF, Naseri N, Khodadadi I, et al. Toxicity and hepatoprotective effects of ZnO nanoparticles on normal and high-fat diet-fed rat livers: mechanism of action. Biol Trace Elem Res. 2025;203(1):199-217. [DOI: 10.1007/s12011-024-04108-5]

[27] Attia H, Nounou H, Shalaby M. Zinc oxide nanoparticles induced oxidative DNA damage, inflammation and apoptosis in rat's brain after oral exposure. Toxics. 2018;6(2):29. [DOI: 10.3390/toxics6020029]

[28] Moatamed ER, Hussein AA, El-Desoky MM, El Khayat ZE. Comparative study of zinc oxide nanoparticles and its bulk form on liver function of Wistar rat. Toxicol Ind Health. 2019;35(10):627-37. [DOI: 10.1177/0748233719878970]

[29] Kian M, Soleimanzadeh A, Javadi S, Najafi G. Efficacy of zinc oxide nanoparticles in chemical castration of male Wistar rats. Sci Rep. 2025;15:44702. [DOI: 10.1038/s41598-025-28667-2]

[30] Liu S, Zhou H, Shi Y, Yi S, Wang X, Li J, Liao B, Cao J, Li G. Zinc oxide nanoparticles induce renal injury by initiating oxidative stress, mitochondrial damage and apoptosis in renal tubular epithelial cells. Biol Trace Elem Res. 2024;202(2):481-92. [DOI: 10.1007/s12011-023-03683-3]

[31] Ghareeb OA, Ali QA. Pathotoxic impact of zinc oxide nanoparticles on liver function and protective role of Silymarin. Curr Innov Dis Health Res. 2023;3:153-61. [DOI: 10.9734/bpi/cidhr/v3/10703F]

[32] Al-Azawi RS, Al-Shukri HH, Ali SH, Abbas SM, Ibraheem NJ, Al-Alwany EAH. Study of the effects of high protein intake on TCF7L2 gene expression and physiological antioxidant enzymes in liver of rat model. Agric Biotechnol J. 2026;18(2):395-414. [DOI: 10.22103/JAB.2026.26796.1846]

[33] Chabuk HAH, Mohammed W. The protective impact of aqueous ginger extract on oxidative stress and inflammation of the male rats' lungs exposed to cigarette smoke. Scientifica. 2026;2026:1214459. [DOI: 10.1155/sci5/1214459]